ISBN: 978-3-95450-236-3 ISSN: 2673-7027 doi:10.18429/JACoW-eeFACT2022-TUZAS0101

LONGITUDINALLY POLARIZED COLLIDING BEAMS AT THE CEPC*

Z. Duan†, T. Chen[1], W. H. Xia[1], J. Gao[1], D. H. Ji, X. P. Li, D. Wang, Y. W. Wang, J. Q. Wang[1]
Key Laboratory of Particle Acceleration Physics and Technology,
Institute of High Energy Physics, Chinese Academy of Sciences, Beijing, China
[1]also at University of Chinese Academy of Sciences, Beijing, China

Abstract

This paper reports the recent progress in the design studies of longitudinally polarized colliding beams for the Circular Electron Positron Collider (CEPC). The overall design concept is outlined, followed by more detailed descriptions of the polarized beam generation, polarization maintenance in the booster, and spin rotators in the collider rings.

INTRODUCTION

The Circular Electron Positron Collider (CEPC) [1, 2] is a next generation electron-positron circular collider, working at center-of-mass energies of 91 GeV (Z-factory), 160 GeV (W- factory), 240 GeV (Higgs-factory), upgradable to 360 GeV (ttbar energy), and aiming at ultra-high precision measurements and probe into new physics beyond Standard Model. The resonant depolarization technique (RD) [3] is essential for precision measurements of the mass of Z and W bosons, this requires transversely polarized e^+ and e^- beams with at least 5% to 10% beam polarization. Meanwhile, probing the spin dimension with longitudinally polarized colliding beams can be very beneficial to enhance particular channels, reduce background and facilitate searches for beyond Standard Model chiral new physics. This application requires 50% or more longitudinal polarization (for e- beam alone, or for both beams) at the Interaction Points (IPs) as well as a high luminosity. These applications demand a careful study of the polarized beam generation and maintenance as well as spin manipulation in the collider rings.

Top-up injection will be adopted in the CEPC collider rings, to maximize the integrated luminosity. In this operation mode, the time-averaged beam polarization $P_{\rm avg}$ of the colliding beams contains two different contributions, one is from the Sokolov-Ternov effect [4] in the storage ring, characterized by the equilibrium beam polarization $P_{\rm DK}$, the other is from the injected beam polarization $P_{\rm inj}$,

$$P_{\rm avg} = \frac{P_{\rm DK}}{1+\tau_{\rm DK}/\tau_{\rm b}} + \frac{P_{\rm inj}}{1+\tau_{\rm b}/\tau_{\rm DK}} \quad (1)$$

where $\tau_{\rm b}$ is the beam lifetime, which is mainly limited by the radiative Bhabha effect and is correlated to the luminosity. $\tau_{\rm DK}$ is the polarization build-up time, $\tau_{\rm DK}^{-1} = \tau_{\rm BSK}^{-1} + \tau_{\rm dep}^{-1}$, where $\tau_{\rm BSK}$ and $\tau_{\rm dep}$ are the time constants characterizing the Sokolov-Ternov effect and the radiative depolarization effect [5], respectively. The equilibrium beam polarization $P_{\rm DK}$ [6] can be approximated by

$$P_{\rm DK} \approx \frac{P_\infty}{1+\frac{\tau_{\rm BKS}}{\tau_{\rm DK}}} \quad (2)$$

where P_∞ is the equilibrium beam polarization taking into the orbital imperfections, but disregarding the radiative depolarization effect, $P_\infty = 92.4\%$ in an ideal planar ring, and is generally lower in an imperfect ring.

If a highly polarized beam is injected into the collider ring, and in the case of $\tau_{\rm b} \ll \tau_{\rm DK}$, the time-averaged beam polarization of the colliding beams can be evaluated by

$$P_{\rm avg} \approx \frac{P_{\rm inj}}{1+\frac{\tau_{\rm b}}{\tau_{\rm BKS}}\frac{P_\infty}{P_{\rm DK}}} \quad (3)$$

this indicates that a very low level of $P_{\rm DK}$ would reduce $P_{\rm avg}$. In Table 1, we assume $P_{\rm inj} = 80\%$, and calculate the required minimum $P_{\rm DK}$ to reach $P_{\rm avg} \geq 50\%$. Given the relative ratio between $\tau_{\rm b}$ and $\tau_{\rm BKS}$, a larger $P_{\rm DK}$ is required at a higher beam energy, which poses a greater challenge in the mitigation of the radiative depolarization effect in the collider rings. Nevertheless, injection of highly polarized beams into the collider rings, has the potential of reaching a high level of $P_{\rm avg}$ besides a high luminosity, and is essential to realize longitudinally polarized colliding beams.

Table 1: CEPC Beam Parameters Related to $P_{\rm avg}$

Beam energy	**45.6 GeV Z**	**80 GeV W**	**120 GeV Higgs**
$\tau_{\rm b}$(hour)	2.5	1.4	0.43
$\tau_{\rm BKS}$(hour)	256	15.2	2.0
$P_{\rm DK,min}$	0.6%	5%	11%

In addition, pilot non-colliding bunches might be necessary for RD measurements, since the beamstruhlung of colliding bunches substantially increases the rms beam energy spread and could limit the achievable accuracy of RD measurements. These pilot bunches operate in the decay mode, and the Sokolov-Ternov effect [4] can be used to generate the required polarization for RD measurements, where asymmetric wigglers [7] are required to boost the self-polarization process at Z-pole [8]. Nevertheless, injection of highly polarized beams into these pilot bunches could be a viable alternative approach for RD measurements as well.

Figure 1 shows the envisaged modification of the CEPC accelerator complex to implement polarized beams. Electron beam with over 80% polarization can be generated from

* Work supported by National Natural Science Foundation of China (Grant No. 11975252); National Key Program for S&T Research and Development (Grant No. 2016YFA0400400 and 2018YFA0404300); Key Research Program of Frontier Sciences, CAS (Grant No. QYZDJ-SSW-SLH004); Youth Innovation Promotion Association CAS (No. 2021012)
† zhe.duan@ihep.ac.cn

ISBN: 978-3-95450-236-3 ISSN: 2673-7027 doi:10.18429/JACoW-eeFACT2022-TUZAS0101

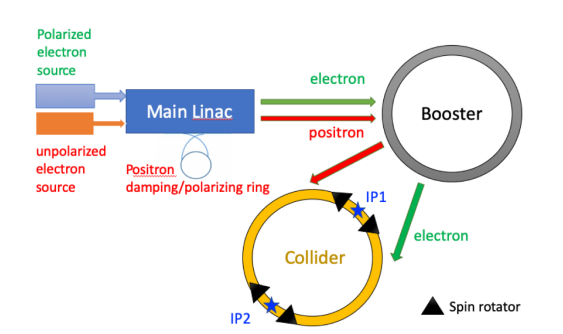

Figure 1: The envisaged modification of the CEPC accelerator complex to implement polarized beams.

the polarized electron source [9], while polarized positron source is more technically challenging [10]. We propose to implement asymmetric wigglers [7] in the positron damping ring, this would generate over 20% beam polarization within 10 minutes, sufficient for RD measurements. Then, the polarized beams are transferred through the injection chain, though it is worried that severe depolarization could occur in the booster where many spin resonances are crossed during the acceleration process, our study shows that the highly periodic lattice structure features weaker spin resonances than expected, and the depolarization could be manageable. We've also implemented a pair of spin rotators around each IP in the CEPC collider ring for the Z-pole energies, which is essential for longitudinally polarized colliding beams.

POSITRON DAMPING/POLARIZING RING

In the injector design in the CEPC CDR [1], 3 nC unpolarized positron bunches are converted from the interaction of a 4 GeV, 10 nC unpolarized primary electron bunch with a target, after pre-acceleration, they are injected into a positron damping ring to reach the desired beam quality for later transportation. By default, 4 positron bunches will stay in the positron damping ring for 20 ms, to satisfy the needs to fill the colliding bunches, In this case, the extracted bunches are unpolarized. The possibility to polarize the positron bunches using the Sokolov-Ternov effect [4] in the positron damping ring [11] or another dedicated ring of similar size [12] have been considered before. This requires very strong asymmetric wigglers to polarize all the positron bunches and satisfy the timing needs to fill all colliding bunches, which is very challenging. However, it is more feasible to generate polarized positron bunches to satisfy the needs of RD measurements. Assume we store one or two positron bunches in the positron damping ring for a longer time, say 10 min, in addition to the other bunches that supply the top-up injection. If we aim at generation of over 20% beam polarization, we need to achieve a self-polarization build-up time τ_{DK} of about 30 min.

Figure 2 shows the layout of a candidate lattice of the positron damping ring. In this design, the blue region represents the lattice sections that can hold up to 24 m total

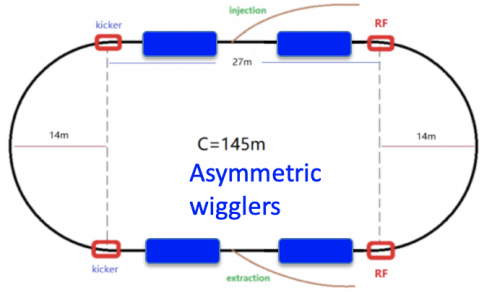

Figure 2: A schematic plot of a candidate lattice of the positron damping ring.

length of asymmetric wigglers. Some tentative parameters are summarized in Table 2. The magnetic fields of the inner and outer parts of an asymmetric wiggler are 1.8 T and -0.36 T, respectively. More detailed evaluation of the influence of the wigglers to the lattice performance is under way. This scheme is compatible with the top-up injection timing needs for the injector, and could supply one or two polarized positron bunches every 10 min for RD measurements in the positron collider ring.

Table 2: Beam Parameters of Positron Damping Ring

Parameter	Value
Beam energy, $G\gamma$	1.542 GeV, 3.5
Circumference	145 m
Wiggler magnetic field B_+/B_-	1.8 T/0.36 T
Wiggler total length	24 m
P_∞ w/ wigglers	90%
τ_{BKS} w/o wigglers	52 min
τ_{BKS} w/ wigglers	34 min
Store time	10 min
Polarization of extracted beam	22%

POLARIZED BEAM ACCELERATION

As the beam energy ramps in an electron (positron) booster ring, so is the closed orbit spin tune ν_0 and the amplitude-dependent spin tune ν_s among beam particles since $\nu_s \approx \nu_0 \approx a\gamma$, $a = 0.00115965$ for electron and positron, γ is the Lorentz factor. This leads to crossing of the underlying spin resonances and could lead to beam depolarization. The polarization loss during crossing of a single, isolated spin resonance can be estimated with the Froissart-Stora formula [13]: $P_f/P_i = 2e^{-\frac{\pi|\epsilon|^2}{2\alpha}} - 1$, where P_i and P_f are the beam vertical polarization before and after crossing the resonance, ϵ is the spin resonance strength, $\alpha = \frac{da\gamma}{d\theta}$ is related to the energy ramping rate. There are three parameter regimes of $|\epsilon|/\sqrt{\alpha}$: the "adiabatic crossing" regime, if $|\epsilon|/\sqrt{\alpha} > 1.84$, then the depolarization is less than 1% but with a "spin-flip"; the "fast crossing" regime, if $|\epsilon|/\sqrt{\alpha} < 0.056$ then the depolarization is also less than 1%; the "intermediate" regime, $0.056 < |\epsilon|/\sqrt{\alpha} < 1.84$, a

ISBN: 978-3-95450-236-3 ISSN: 2673-7027 doi:10.18429/JACoW-eeFACT2022-TUZAS0101

stronger depolarization occurs. There are two families of important spin resonances in this context: the imperfect resonances $\nu_0 = k, k \in Z$, mainly driven by horizontal magnetic fields due to vertical orbit offsets in quadrupoles and dipole roll errors, and the intrinsic resonances $\nu_0 = k \pm \nu_y, k \in Z$ with ν_y the vertical betatron tune, driven by the horizontal magnetic field due to vertical betatron oscillations in quadrupoles. Adjacent imperfection resonances are spaced by 440 MeV, and it is clear hundreds of spin resonances of these two families will be crossed in the acceleration of CEPC booster from injection energy at 10 GeV to extraction energies of 45.6 GeV, 80 GeV and 120 GeV.

Previous studies suggested using Siberian snakes [12, 14] in these 100 km electron boosters to mitigate the depolarization. However, the practical implementations of snakes using either bending magnets or solenoids are cumbersome in size and costs. A concept of "spin-resonance free electron ring injector" [15] was proposed in the study of the Electron Ion Collider [16]. A booster lattice with a high effective periodicity of 96 was designed, so that supper strong spin resonances are all beyond the top energy at 18 GeV, while the other spin resonances are generally weak, well within the "fast crossing" regime and severe depolarization is thus avoided. This work emphasizes on the importance of the spin resonance structure.

We carefully examined the spin resonance structure of the CEPC CDR booster lattice. It features a super-periodicity of $P = 8$ with interleaved arc and straight sections. Each arc section contains $M = 99$ FODO cells with 90 degree betatron phase advances, the vertical betatron tune is $\nu_y = 261.2$, and the total contribution from all arc sections to the vertical betatron tune is $\nu_B = 198$. A similar model ring lattice was studied in Ref. [17], where analytical estimations of the spin resonance strengths and their structure were obtained. It was shown that the contributions from all arc FODO cells add up near super strong spin resonances. The super strong imperfection resonances are located at $\nu_0 = nPM \pm [\nu_B]$, while the super strong intrinsic resonances are located at $\nu_0 = nP \pm \nu_y$ near $nPM \pm [\nu_B]$, where $[x]$ denotes the integer part of x. However, regular spin resonances away from these conditions are generally weak due to cancellation. Application of this theory to the CEPC booster lattice indicates that it has effectively a very large super-periodicity of $PM = 792$, and the first super strong resonances are located near $\nu_0 = [\nu_B] = 198$, other super strong resonances are well beyond the working beam energies of the CEPC booster.

To verify this analysis, we calculated the spin resonance spectrum of the CEPC booster lattice in the working beam energy range, as shown in Fig. 3. The DEPOL code was employed to calculate the intrinsic spin resonance strengths at a vertical normalized emittance of 10πmm $\cdot$ mrad. The super strong intrinsic resonances are near $G\gamma = 198$, between the working energies for W and Higgs, other resonances are much weaker. To evaluate the imperfection spin resonance spectrum, we introduced magnetic field errors and misalignment errors to dipoles, quadrupoles and sextupoles. The main contribution of closed orbit distortion is from the 100 μm rms misalignment error in quadrupoles, we then implemented closed orbit corrections and betatron tune corrections. For this study, we use a imperfect lattice seed after correction with a vertical rms closed orbit distortion of about 100μm. We numerically evaluated the strength of the imperfection resonance $\nu_0 = k$ via $\epsilon_k \approx \frac{1+k}{2\pi} \sum_{h=1}^{M} [p_{y,0}(s_{h,2}) - p_{y,0}(s_{h,1})] e^{ik\Phi(s_{h,1})}$, where we replace the integral by a sum over M magnet elements in the lattice, $s_{h,1}$ and $s_{h,2}$ are the longitudinal positions of the entrance and the exit of the h-th magnet, respectively, $p_{y,0}$ is the vertical canonical momentum on the closed orbit, $\Phi(s) = \frac{1}{\nu_y} \int_0^s \frac{1}{\beta_y(s)} ds$. The imperfection resonance strengths generally increase with energy besides the super strong resonance near $a\gamma = 198$. Apart from the super strong intrinsic resonance and a few imperfection resonances at higher energies, the resonance crossings of most spin resonances are well within the "fast-crossing" regime so that depolarization is very small.

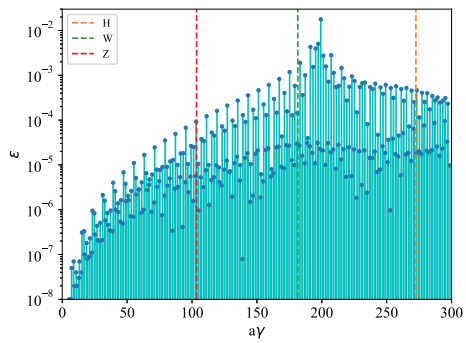

(a) Intrinsic resonances

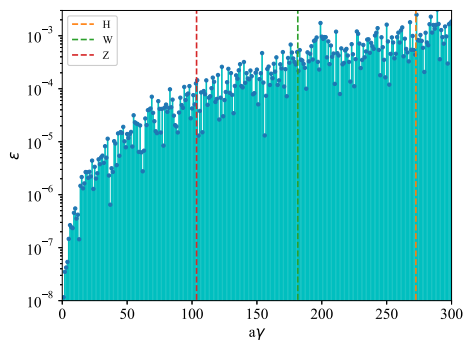

(b) Imperfection resonances

Figure 3: The spectra of intrinsic (upper) and imperfection (lower) spin resonances of an imperfect seed of the CEPC CDR booster lattice. The intrinsic resonances are calculated for a vertical normalized emittance of 10πmm $\cdot$ mrad. The three vertical dashed lines indicate the three extraction energies.

We launched simulations of the beam polarization transmission in the energy ramping process using the long term tracking capability of Bmad [18]. A cosine shape energy

ISBN: 978-3-95450-236-3 ISSN: 2673-7027 doi:10.18429/JACoW-eeFACT2022-TUZAS0101

ramping curve was adopted, $E(t) = E_{\text{inj}} + \frac{(E_{\text{ext}} - E_{\text{inj}})}{2}(1 - \cos(\frac{\pi t}{t_{\text{ramp}}}))$. The booster injection energy was fixed to 10 GeV, and the ramping time t_{ramp} was set to 1.9 s, 3.3 s and 5.0 s for the acceleration to the extraction energy 45.6 GeV (Z), 80 GeV (W) and 120 GeV (H), respectively. The RF voltages and phases are set to compensate for the synchrotron radiation energy loss, as well as maintain a fixed synchrotron tune of 0.1, 0.1, and 0.13 for the three extraction energies, respectively. The injected beam is modeled with 1000 particles in a 6D Gaussian distribution. Following the CEPC CDR parameters [1], the rms horizontal and vertical emittances are set to 80 nm and 40 nm, respectively. The rms energy spread and bunch length are set to 0.16% and 1 mm, respectively. The beam particles are initialized with a 100% vertical polarization, during the tracking the vertical polarization of the beam is calculated as the ensemble average of the vertical spins of the particles. Fig. 4 shows the evolution of the vertical beam polarization in the acceleration to the three different extraction energies. In both the cases of Z and W energies, the polarization loss is less than 5%. In contrast, in the case of Higgs energy, there is almost 40% polarization loss when crossing the super strong intrinsic resonance near $\nu_0 = 198$, and another 10% polarization loss due to resonance crossings at even higher beam energies. In principle, the impact of the super strong intrinsic resonance can be partially mitigated by a dedicated correction of the vertical equilibrium emittance, or improve the lattice design so that the first super strong resonances are beyond the whole working energy range.

These preliminary studies suggest it is possible to largely maintain the beam polarization in the acceleration process to 45.6 GeV and 80 GeV, without Siberian snakes. More detailed study of the influence of machine imperfections is under way.

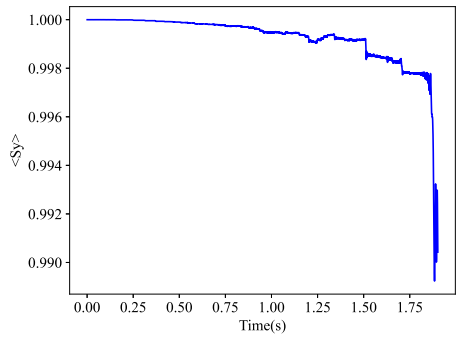

(a) Acceleration to 45.6 GeV

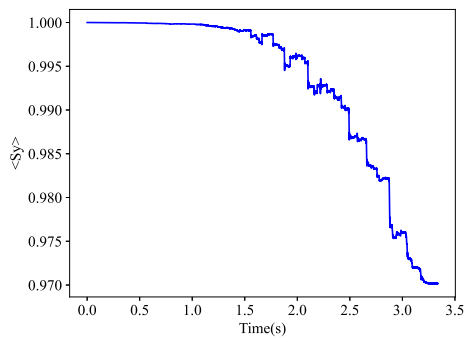

(b) Acceleration to 80 GeV

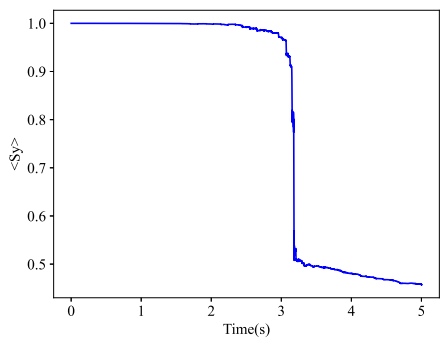

(c) Acceleration to 120 GeV

Figure 4: Simulated evolution of the vertical beam polarization in the acceleration to Z (upper), W (middle) and Higgs (lower) energies.

SPIN ROTATORS IN THE COLLIDER RING

To realize the longitudinal polarization at IPs in the electron collider ring, a pair of spin rotators need to be inserted around each of the two IPs. This helps maintain vertical polarization in most part of the collider ring, and thus avoids significant depolarization. The detailed design of the spin rotators is reported elsewhere [19]. Here, we'll summarize the main results, and focus on the case that the spin rotator is only implemented in the electron collider ring.

Each spin rotator consists of a bending magnet section and a solenoid magnet section. The total spin rotation angle in each bending magnet section from the IP to each solenoid section needs to be an odd multiple k of $\pi/2$ to rotate the spins from the longitudinal to the radial direction, which corresponds to an orbital bending angle of at least 15.18 mrad at 45.6 GeV. Then, the solenoid section need to rotate the spin from the radial to vertical direction. The required solenoid integral strength is about 240 T·m to rotate the spin vector by $\pi/2$ at a beam energy of 45.6 GeV. This corresponds to a total length of 30 m for superconducting solenoid magnets of 8 T. The solenoid magnets are interleaved by quadrupoles to compensate for the transverse coupling [20]. The layout of a pair of spin rotators around one IP is illustrated in Fig. 5. The S-shape geometry in the interaction region is utilized in the arrangement of the spin rotators, which are just placed out of the interaction region [14, 21]. The half crossing angle at the IP is 16.5 mrad, addition bending magnet sections ($\Delta\theta_1$ and $\Delta\theta_2$) are required in both spin rotators, next to the solenoid sections. In the counterpart region of the positron collider ring, the solenoid sections are replaced by straight sections with quadrupoles to match the optics. The circumference increases by about 2 km, the betatron

ISBN: 978-3-95450-236-3 ISSN: 2673-7027 doi:10.18429/JACoW-eeFACT2022-TUZAS0101

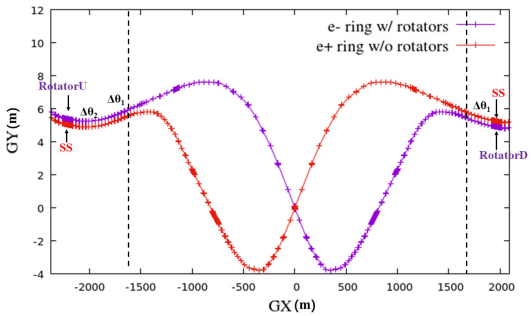

Figure 5: Geometry of the electron and positron collider rings near one interaction region [19], with solenoid spin rotators (RotatorU and RotatorD) for the electron beam, and compensating straight sections (SS) for the positron beam.

tunes increase by 10 units, while other beam parameters almost remain unchanged. Simulations also indicate there is only a moderate shrink of dynamic aperture, which can be recovered via dedicated optimizations.

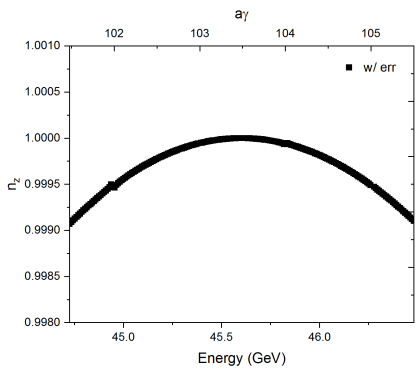

Figure 6: Longitudinal projection of $\mathbf{n_0}$ at the IP for different beam energies, for the lattice with magnet errors.

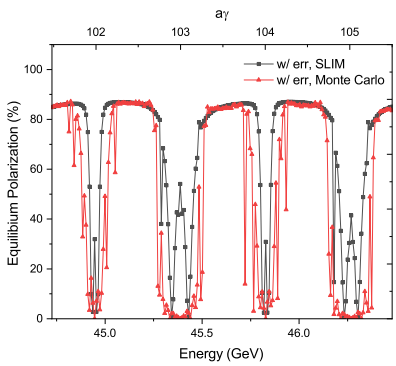

Figure 7: Comparsion of the equilibrium beam polarization for the lattice with spin rotators in the presence of magnet errors, simulated using the SLIM algorithm in Bmad and the Monte Carlo simulation in PTC, respectively. The step size $\Delta a\gamma = 0.02$.

We also numerically evaluated the performance of the spin motion using the BMAD/PTC code [18, 22]. In a realistic storage ring, the solenoid magnetic field may be not perfectly compensated due to magnets' errors. These magnet errors also drive spin resonances and lead to a reduced equilibrium beam polarization. We introduced in the solenoid sections relative field errors for solenoids and quadrupoles with a root-mean-squared value of 0.05%, and relative roll errors for quadrupoles with a root-mean-squared value of 0.01%. Fig. 6 shows the simulated longitudinal projection of the $\vec{n}_0$-axis at one IP, for different beam energies. Such an "anti-symmetric" spin rotator design is not very sensitive to a variation of the beam energy. Fig. 7 shows the simulated equilibrium beam polarization using the SLIM algorithm [23] in BMAD [18], and Monte-Carlo simulations implemented in PTC [24]. These simulations show clear depolarization near major spin resonances, the Monte-Carlo simulations also indicate the influence of higher-order synchrotron sideband spin resonances, absent from the SLIM simulations. Nevertheless, there are still sufficient safe space with fractional part of $a\gamma$ near 0.5, where the equilibrium beam polarization is very high. These simulations shows the robustness of the "anti-symmetric" spin rotator design against machine imperfections.

Next, we'll introduce other kinds of machine imperfections into the lattice with spin rotators, and evaluate the influence on the performance of the orbital and spin motion.

CONCLUSION

This paper summarizes the recent progress in the design studies of longitudinally polarized colliding beams at the CEPC. Generation of polarized beams from the source and injection into the collider rings are studied. It is proposed that positron bunches with over 20% polarization can be generated in the positron damping ring, to fit the needs of resonant depolarization. Our studies suggest beam polarization could be well preserved in the booster up to 45.6 GeV and even higher energies, without Siberian snakes. Spin rotators have also been implemented in the collider rings at Z-pole with promising performance. More technical aspects of these studies and potential extension to higher beam energies are under way.

Note that injected polarized electron and positron beams could also benefit RD measurements. Compared to the approach using self-polarization [8] with the help of asymmetric wigglers, the polarization level can be much higher, there is no initial dead time for physics, RD measurements can be conducted more frequently for at least the electron beam. It is also possible to carry out RD measurements on colliding bunches, especially at lower bunch charge. More quantitative evaluation of these aspects is planned.

ACKNOWLEDGEMENTS

The authors are grateful to D. P. Barber and S. Nikitin for helpful discussions, and D. Sagan and E. Forest for the kind help with simulation codes Bmad/PTC.

ISBN: 978-3-95450-236-3 ISSN: 2673-7027 doi:10.18429/JACoW-eeFACT2022-TUZAS0101

REFERENCES

[1] The CEPC Study Group, "CEPC Conceptual Design Report Volume I-Accelerator," *arXiv:1809.00285v1 [physics.acc-ph]*, 2018, doi:10.48550/arXiv.1809.00285

[2] The CEPC Accelerator Study Group, "Snowmass2021 White Paper AF3-CEPC," *arXiv:2203.09451*, 2022, doi:10.48550/arXiv.2203.09451

[3] Y. S. Derbenev, A. M. Kondratenko, S. I. Serednyakov, *et al.*, "Accurate calibration of the beam energy in a storage ring based on measurement of spin precession frequency of polarized particles," *Part. Accel.*, vol. 10, p. 177, 1980.

[4] A. A. Sokolov and I. M. Ternov, "On polarization and spin effects in the theory of synchrotron radiation," *Sov. Phys. Dokl.*, vol. 8, p. 1203, 1964.

[5] V. N. Baier and Y. F. Orlov, "Quantum depolarization of electrons in a magnetic field," *Sov. Phys. Dokl.*, vol. 10, p. 1145, 1966.

[6] Y. S. Derbenev and A. M. Kondratenko, "Diffusion of Particle Spin in Storage Rings," *Sov. Phys. JETP*, vol. 35, pp. 230–236, 1972.

[7] A. Blondel and J. M. Jowett, "Wigglers for polarization," *Conf. Proc. C8711093*, vol. 216, 1987.

[8] A. Blondel, P. Janot, J. Wenninger, *et al.*, "Polarization and Centre-of-mass Energy Calibration at FCC-ee," *arXiv:1909.12245 [hep-ex, physics:physics]*, 2019, doi:10.48550/arXiv.1909.12245

[9] A. Brachmann *et al.*, "The polarized electron source for the international collider (ILC) project," in *AIP Conference Proceedings*, vol. 915, 2007, pp. 1091–1094, doi:10.1063/1.2750959

[10] P. Musumeci, *et al.*, "Positron sources for future high energy physics colliders," *arXiv:2204.13245 [physics]*, 27, 2022, doi:10.48550/arXiv.2204.13245

[11] Z. Duan *et al.*, "Concepts of longitudinally polarized electron and positron colliding beams in the Circular Electron Positron Collider," *in Proc. of IPAC'19,*, Melbourne, Australia, May 2019, pp. 445-448., doi:10.18429/JACoW-IPAC2019-MOPMP012

[12] I. A. Koop, A. V. Otboev, and Y. M. Shatunov, "Ideas for longitudinal polarization at the Z/W/H/top factory," *Proc. eeFACT 2018, WEXAA04*, p. 190, 2018, doi:10.18429/JACoW-eeFACT2018-WEXAA04

[13] M. Froissart and R. Stora, "Depolarisation d'un faisceau de protons polarises dans un synchrotron," *Nucl. Instrum. Methods*, vol. 7, no. 3, pp. 297–305, 1960, doi:10.1016/0029-554X(60)90033-1

[14] S. A. Nikitin, "Polarization issues in circular electron–positron super-colliders," *Int. J. Mod. Phys. A*, vol. 35, no. 15&16, 2020, doi:10.1142/S0217751X20410018

[15] V. H. Ranjbar *et al.*, "Spin resonance free electron ring injector," *Phys. Rev. Accel. Beams*, vol. 21, p. 111 003, 2018, doi:10.1103/PhysRevAccelBeams.21.111003

[16] F. Willeke and J. Beebe-Wang, "Electron Ion Collider Conceptual Design Report 2021," Tech. Rep. BNL-221006–2021-FORE, 1765663, 2021, doi:10.2172/1765663

[17] S. Y. Lee, *Spin dynamics and snakes in synchrotrons*. World Scientific, 1997, doi:10.1142/3233

[18] D. Sagan *et al.*, "The Bmad Reference Manual," https://www.classe.cornell.edu/bmad/manual.html.

[19] W. Xia, Z. Duan, J. Gao, and Y. Wang, "Investigation of spin rotators in CEPC at the Z-pole," *Radiat. Detect. Technol. Methods*, vol. 6, no. 4, pp. 490–501, 2022, doi:10.1007/s41605-022-00344-2

[20] D. P. Barber, J. Kewisch, G. Ripken *et al.*, "A solenoid spin rotator for large electron storage rings," *Part. Accel.*, vol. 17, pp. 243–262, 1985.

[21] S. A. Nikitin, "Opportunities to obtain polarization at CEPC," *Int. J. Mod. Phys. A*, vol. 34, no. 13&14, p. 1 940 004, 2019, doi:10.1142/S0217751X19400049

[22] E. Forest, F. Schmidt, and E. McIntosh, "Introduction to the Polymorphic Tracking Code," *CERN-SL-2002-044 (AP), and KEK-Report 2002-3*, 2002.

[23] A. Chao, "Evaluation of radiative spin polarization in an electron storage ring," *Nucl. Instrum. Methods Phys. Res.*, vol. 180, p. 29, 1981.

[24] Z. Duan, M. Bai, D. P. Barber, and Q. Qin, " A Monte-Carlo simulation of the equilibrium beam polarization in ultra-high energy electron (positron) storage rings," *Nucl. Instrum. Methods Phys. Res., Sect. A*, vol. 793, pp. 81–91, 2015, doi:10.1142/S0217751X19400049